144 KSME Journal, Vol. 7, No. 2, pp. 144~157, 1993

Study of Unsteady Fluid-Dynamic Forces Acting on a Flexible Cylinder in a Concentric Annulus

W.-G. Sim* and Y. C. Cho**

(Received November 9, 1992)

The unsteady fluid-dynamic forces, generated by a flexural motion in axial (laminar) flow, have been formulated based on a collocation finite-difference method for concentric configurations, in connection with the flow-induced vibration problem. Based on the numerical method, the governing equations of the unsteady flow, obtained from the appropriate Navier-Stokes and continuity equations, redcuced to a system of algebraic equations leading to a block-tridiagonal system. To obtain a solution of the system, the LU decomposition method is used considering the factorization scheme. This numerical method is capable of taking fully into account unsteady viscous effects and of predicting viscous forces rigorously rather than approximately, in contrast with existing theories. In order to validate the numerical approach, semi-analytical approaches have been developed for estimating the fluid-dynamic forces. The numerical results are compared to the analytical results and good agreement was found. The contribution of unsteady viscous damping forces to the overall unsteady forces is significant for low values of the oscillatory Reynolds number, expecially in very narrow annuli.

Key Words: Flow-Induced Vibration, Added Mass, Viscous Damping, Hydrodynamic Force, Oscillatory Reynolds Number

1. Introduction

When a structure submerged in fluid oscillates, the surrounding fluid must be displaced to accommodate the motion of the structure. There is generally fluid-structure coupling and interaction. Sometimes, fluid flow around the structure has the potential to cause destructive vibrations. Hence, the study of flow-induced vibrations is of great interest for design. The interested reader is referred to Chen's(1981) and Païdoussis's(1987) reviews on flow-induced vibration and instabilities. For the future purpose to predict the critical flow velocity where system loses stability, the hydrodynamic forces associated with the motion of the flexible cylinder are formulated in the present paper.

The dynamics of a flexible cylinder subjected to steady axial flow was first investigated by Païdoussis, both theoretically (1966a) and experimentally (1966b), for the system in unconfined flow. The coupled-hydrodynamic forces acting on the cylinder was formulated according to slender body theory, as proposed by Lighthill(1960) for inviscid fluid, and the viscous forces were formulated by simple linerarized relationships, earlier proposed by Taylor(1952). In general, the added mass, which is associated with inertia forces, has a significant effect on the natural frequencies of system, while hydrodynamic stiffness effects are responsible for the onset of fluid-elastic instability by divergence. On the other hand, negative flow-induced damping is responsible for flutter.

* Auxiliary Systems Design Dept, Korea Atomic Energy Reserch Institute, P.O. Box 7, Deaduk-danji, Taejeon, 305-606, Korea

** Department of Mechanical Engineering Inha University, Inchon, 402-751, Korea

In a subsequent patper (Païdoussis, 1973), the theory was extended to confined viscous flow considering the effect of confinement of the fluid flow by a duct, in which the formulation of the viscous forces was adjusted appropriately and the gravity and pressurization effects were taken into account. The virtual mass of the confined fluid flow associated with the lateral motions of the system becomes large and the system loses stability much earlier, but the fundamental behaviour is not altered. The theory was validated by comparison with the experimental results (Païdoussis and Pettigrew, 1979), where it was found that, with increasing flow velocity, the cylinder is subject, sequentially, to instabilities of increasing mode number, confinement severely destabilizing the system.

In most of the previous studies, the fluid-dynamic forces acting on the oscillating cylinder subjected to axial flow have been developed based on uniform axial flow. Therefore, the effect of laminar axial flow is still difficult to quantify systematically. In this work, the fluid-dynamic forces have been formulated from the Navier-Stokes equations, accounting for unsteady viscous flow effects much more fully than the semi-empirical and approximate formulations utilized heretofore.

In an attempt to predict the fluid-dynamic forces acting on a cylinder surrounded by a viscous or an inviscid fluid in an eccentric annulus, the spectral collocation method has first been applied to system having "translational motion" in quiescent fluid, where "translational motion" is understood to mean motion transverse to the flow, such that the sides of the two cylindrical bodies remain parallel to each other (Sim and Cho, 1993). In the present work, the spectral collocation method is used to solve the three-dimensional problem for a system having flexural motion in a concentric annulus conveying viscous axial flow ; in this case, the specitral collocation method have been modified and used together with the finite-difference method in a hybrid scheme (Patanker, 1980). In the present paper, this method is called the collocation-finite-difference method. As a result, the fluid-dynamic forces including the viscous effects can be evaluated rigorously rather than approximately, in contrast with existing theories.

The fluid-dynamic forces acting on a flexible cylinder, as influenced by the axial steady flow (laminar flow), are calculated by this collocation finite-difference method. Considering the previous analytical theory (Païdoussis, et al., 1990) and utilizing the spectral collocation method, the semi-analytical theory is developed for estimating the unsteady fluid dynamic forces. The semi-analytical method is less restricted to very narrow annuli, as compared to the analytical solution. The numerical results are discussed and compared with the semi-analytical results in order to validate the present numerical approach.

The inner cylinder is assumed to have a simple flexural motion, as a clamped-clamped beam. In order to simplify the problem and to get general information, only the first of the modes of the beam is considered for the oscillatory motion of the flexible cylinder, This cylinder has length L and radius a. The radius of outer cylinder is b ; hence the annular space between two cylinders is $H=b-a$. The motions are assumed to be small.

2. Collocation Finite-Difference Method

When a system of equations is obtained by the collocation method with nth order of interpolation functions for axial variation, the discretized-system equations might become n times larger than those of pure two-dimensional problem, where the same number of collocation points are selected for the radial and circumferential coordinates. As shown in the previous study (Sim and Cho, 1993), the solutions given by the spectral method converged fast. However, difficulties are encountered in the three-dimensional problem due to a relatively large full matris system, which might produce singularity problems in the mathematical procedure. In order to avoid this difficulty, a finite difference method based on a hybrid scheme is adapted for axial variations, which is characterized by an artificial viscosity contributing to achieve convergence of the solution.

The hybrid scheme is related only to the axial domain, while the collocation method is used for the radial and circumferential domains. As a result, the axial domain is subdivided into a certain number of grid points, where spectral expansions for the fluid parameters are defined. The numerical details of the collocation method, which remain the same as for the two-dimensional flow discussed in the previous study (Sim and Cho, 1993), have not been repeated in this paper. However, an attempt has been made to clearly point out and emphasize the details of the finite-difference method for the present analysis.

Far upstream, the axial flow in fully developed and its velocity can be calculated by author (Mateescu, et al., 1990) using the spectral method. Details of this analysis are omitted here for brevity. In order to formulate the unsteady viscous problem, the results for steady viscous flow are utilized.

2.1 Hybrid method formulation

In this section, the basic concepts needed in the formulation of the hybrid scheme are presented. The hybrid scheme was introduced by Spalding (1972) under the name "High-lateral-flux modification" for the finite difference method. The significance of the hybrid scheme can be understood by observing that it is identical to the central-difference scheme for the mesh Reynolds number range $-2<Re_m(=U\Delta x)/\nu)<2$, and outside this range with an upwind scheme. The axial components of the diffusion terms and convective terms related with the steady axial flow velocity must be considered for the present analysis. The addition these terms does not alter the form of the discretized equations, when the axial derivative terms are relatively small by the assumption of small amplitude motion

Although the convection and diffusion terms connected to the axial variation are the only new terms in this section, its formulation is not very straightforward. The convection term has an inseparable connection with the diffusion term and, therefore, the two terms need to be handled as one unit.

To simplify matters, only the convection and diffusion terms are considered for a one dimensional problem. The governing differential equation is

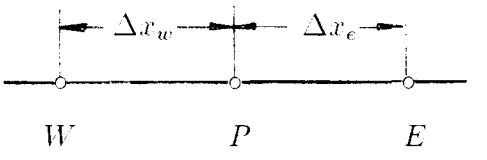

Fig. 1 Typical grid-points cluster for the axial variation

$$\frac{\partial}{\partial x}(\rho Uf)=\frac{\partial}{\partial x}\left(\mu\frac{\partial f}{\partial x}\right), \tag{1}$$

where U represents the steady flow velocity in the axial direction and f denotes any flow field parameter, which will be obtained. As mentioned before, the axial flow velocity, U, can be obtained from Navier-Stokes equations for the steady flow. At this stage, our task is to obtain a solution for f, which will be the unsteady fluid quantities in the present analysis. For concentric configurations, the steady flow velocity does not depend on the axial coordinate consideration.

Using the hybrid scheme, the discretized convective-diffusion equation can be written as

$$a_P f_P = a_E f_E + a_W f_W \text{ if } U>0, \tag{2}$$

where

$$a_E=\frac{\mu}{\Delta x_e}+\|0,\ -\frac{\rho U}{2}\|,$$
$$a_W=\frac{\mu}{\Delta x_w}+\|\rho U,\ \frac{\rho U}{2}\|,$$
$$a_P=a_E+a_W,$$

where $\|p,\ q\|$ represents p for the unwind scheme ($Re_m>2$) or q for the central difference scheme ($-2<Re_m<2$) and the subscripts E and W present east and west wides with respect to the central grid point P in the axial domain. In the present analysis, the axial flow velocity is always positive ; there is no adverse pressure gradient in a constant width annular space.

2.2 Formulation of the system equation for unsteady viscous flow

The inner cylinder surrounded by incompressible viscous fluid flow, has the periodic flexural

motion in a concentric annulus. The vibrating motion is assumed to be simple harmonic, with circular frequency ω. For the three-dimensional problem with steady axial flow, the unsteady governing equations are obtained by subtracting the steady terms from the full Navier-Stokes equations. The linearized Navier-Stokes equations, based on small amplitude motions of the cylinder, and continuity equation in cylindrical coordinates for the present analysis can be reduced

$$\frac{\partial u^*}{\partial t}+v^*\frac{\partial U}{\partial r}+\frac{w^*}{r}\frac{\partial U}{\partial \Theta}+U\frac{\partial u^*}{\partial x}+\frac{1}{\rho}\frac{\partial p^*}{\partial x}$$
$$=\nu\left[\frac{1}{r}\frac{\partial}{\partial r}\left(r\frac{\partial u^*}{\partial r}\right)+\frac{1}{r^2}\frac{\partial^2 u^*}{\partial \Theta^2}+\frac{\partial^2 u^*}{\partial x^2}\right],$$
$$\frac{\partial w^*}{\partial t}+U\frac{\partial w^*}{\partial x}+\frac{1}{\rho}\frac{1}{r}\frac{\partial p^*}{\partial \Theta}=\nu\left[\frac{1}{r}\frac{\partial}{\partial r}\left(r\frac{\partial w^*}{\partial r}\right)\right.$$
$$\left.+\frac{1}{r^2}\frac{\partial^2 w^*}{\partial \Theta^2}+\frac{\partial^2 w^*}{\partial x^2}-\frac{w^*}{r^2}+\frac{2}{r^2}\frac{\partial v^*}{\partial \Theta}\right],$$
$$\frac{\partial v^*}{\partial t}+U\frac{\partial v^*}{\partial x}+\frac{1}{\rho}\frac{\partial p^*}{\partial r}=\nu\left[\frac{1}{r}\frac{\partial}{\partial r}\left(r\frac{\partial v^*}{\partial r}\right)\right.$$
$$\left.+\frac{1}{r^2}\frac{\partial^2 v^*}{\partial \Theta^2}+\frac{\partial^2 v^*}{\partial x^2}-\frac{v^*}{r^2}-\frac{2}{r^2}\frac{\partial w^*}{\partial \Theta}\right], \quad (3)$$
$$\frac{\partial u^*}{\partial x}+\frac{1}{r}\frac{\partial w^*}{\partial \Theta}+\frac{1}{r}\frac{\partial}{\partial r}(rv^*)=0 \quad (4)$$

where u^*, v^* and w^* denote the unsteady flow velocities in the axial, radial and circumferential directions, respectively. In the above equations, the production terms between the unsteady components are neglected for small amplitude motion, and the circumferential variation of steady axial flow is zero for concentric configurations.

Considering the no-slip comdition at the interface between fluid and cylinder, the boundary conditions on the fixed ($r=b$) and moving ($r=a$) cylinders can be expressed as

$$u^*(x, b, \Theta, t)=v^*(x, b, \Theta, t)$$
$$=w^*(x, b, \Theta, t)=0,$$
$$u^*(x, a, \Theta, t)=0,$$
$$v^*(x, a, \Theta, t)=e_v(x, t)\cos\Theta$$
$$=-\frac{\partial e_l(x, t)}{\partial t}\cos\Theta,$$
$$w^*(x, a, \Theta, t)=-e_v(x, t)\sin\Theta$$
$$=-\frac{\partial e_l(x, t)}{\partial t}\sin\Theta, \quad (5)$$

where $e_v(x, t)$ represents the lateral velocity of the moving inner cylinder and $e_l(x, t)$ denotes the corresponding displacement which can be expressed in terms of the eigenfunction $\psi_1(x)$ of the first normal mode for a clamped-clamped beam

$$e_l(x, t)=E(x)e^{\iota\omega t}=a_1\psi_1(x)e^{i\omega t}. \quad (6)$$

The present problem is generalized by the following nondimensional parameters;

$$X=\frac{x}{L},\ l=\frac{L}{a},\ h=\frac{H}{a},\ \hat{U}=\frac{U}{\bar{U}},$$
$$\hat{p}=\frac{p^*}{\rho a^2\omega^2\epsilon_{1/2}e^{\iota\omega t}},\ \hat{u}=\frac{u^*}{\iota a\omega\epsilon_{1/2}e^{\iota\omega t}},$$
$$\hat{v}=\frac{v^*}{\iota a\omega\epsilon_{1/2}e^{\iota\omega t}},\ \hat{w}=\frac{w^*}{\iota a\omega\epsilon_{1/2}e^{\iota\omega t}},$$
$$\hat{e}(X)=\frac{e_v(X, t)}{\iota a\omega e^{\iota\omega t}},\ \hat{e}_r(X)=\frac{\hat{e}(X)}{\hat{e}_{1/2}},$$
$$Re=\frac{\bar{U}2ha}{\nu},\ Re_s=\frac{\omega a^2}{\nu}, \quad (7)$$

where $\hat{e}(X)$ denotes the nondimensional amplitude of velocity or displacement of the moving cylinder, $\bar{U}$ represents the mean axial flow velocity and Re_s is called the oscillatory Reynolds number. As shown in the above equations, the nondimensional unsteady velocities and pressure are defined in terms of $\epsilon_{1/2}=\hat{e}_{1/2}$, where the subscript 1/2 stands for the corresponding local value at $X=1/2$.

In order to transform the annular space (r, Θ) into a rectangular computational domain (Z, $\theta=\Theta$), a convenient coordinate transformation is used using the nondimensional coordinate Z defined as:

$$Z=1-2\frac{r-a}{ah}, \text{ where } ah=H=b-a. \quad (8)$$

Considering the coordinated transformation with the nondimensional parameters, the governing Eqs. (3) and (4), can be rewritten in the computational domain (Z, θ) in the nondimensional form

$$\iota\frac{Re_s}{4}h^2\hat{u}-\iota\frac{Re_s}{4}\frac{h^2}{l}\frac{\partial\hat{p}}{\partial X}+\frac{Re}{8}\left\{\frac{h}{l}\hat{U}\frac{\partial\hat{u}}{\partial X}\right.$$
$$\left.-2\hat{v}\frac{\partial\hat{U}}{\partial Z}\right\}=\left[\frac{\partial^2\hat{u}}{\partial Z^2}-\sqrt{D}\frac{\partial\hat{u}}{\partial Z}\right.$$
$$\left.+D\frac{\partial^2\hat{u}}{\partial\theta^2}+\frac{h^2}{4l^2}\frac{\partial^2\hat{u}}{\partial X^2}\right],$$
$$\iota\frac{Re_s}{4}h^2\hat{w}-\iota\frac{Re_s}{2}h\sqrt{D}\frac{\partial\hat{p}}{\partial\theta}+\frac{Re}{8}\frac{h}{l}\hat{U}\frac{\partial\hat{w}}{\partial X}$$
$$=\left[\frac{\partial^2\hat{w}}{\partial Z^2}-\sqrt{D}\frac{\partial\hat{w}}{\partial Z}+D\frac{\partial^2\hat{w}}{\partial\theta^2}\right.$$

$$+\frac{h^2}{4l^2}\frac{\partial^2\hat{w}}{\partial X^2}-D\left\{\hat{w}-2\frac{\partial\hat{v}}{\partial\theta}\right\}\Big],$$

$$\iota\frac{Re_s}{4}h^2\hat{v}+\iota\frac{Re_s}{2}h\frac{\partial\hat{p}}{\partial Z}+\frac{Re}{8}\frac{h}{l}\hat{U}\frac{\partial\hat{v}}{\partial X}$$
$$=\Big[\frac{\partial^2\hat{v}}{\partial Z^2}-\sqrt{D}\frac{\partial\hat{v}}{\partial Z}+D\frac{\partial^2\hat{v}}{\partial\theta^2}$$
$$+\frac{h^2}{4l^2}\frac{\partial^2\hat{v}}{\partial X^2}-D\left\{\hat{v}+2\frac{\partial\hat{w}}{\partial\theta}\right\}\Big], \tag{9}$$

$$\frac{\partial\hat{v}}{\partial Z}-\sqrt{D}\,\hat{v}-D\frac{\partial\hat{w}}{\partial\theta}-\frac{h}{2l}\frac{\partial\hat{u}}{\partial X}=0, \tag{10}$$

where $D=\{h/[2+h(1-Z)]\}^2$.

In order to get the system equations based on the collocation finite difference method, the non-dimensional parameters can be expressed in terms of Chebyshev polynomials and Fourier expansions. Also, the unknown coefficients are dependent on the axial coordinate. Using the spectral expansion for the flexural motion of the inner cylinder, the following types of expansions can be considered for the fluid-dynamic properties in the three dimensional annular space

$$\hat{u}=\sum_{j=0}^{m}U_j(X)\,T_j(Z)\cos\theta,$$
$$\hat{v}=\sum_{j=0}^{m}V_j(X)\,T_j(Z)\cos\theta,$$
$$\hat{w}=\sum_{j=0}^{m}W_j(X)\,T_j(Z)\sin\theta,$$
$$\hat{p}=\sum_{j=0}^{m-2}P_j(X)\,T_j(Z)\cos\theta, \tag{11}$$

where the unknown coefficients U_j, W_j, V_j and P_j can be decomposed into real and imaginary components.

Taking account of the expaasion forms shown in the above equations, the second of the three Navier-Stokes Eq. (9) and the continuity Eq. (10) can be expressed based on the hybrid scheme as

$$\sum_{j=0}^{m}\begin{pmatrix} W_j[\,T_j''(Z)-\sqrt{D}\,T_j'(Z)-2DT_j(Z) \\ -\iota\frac{Re_s}{4}h^2T_j(Z)-\left(\frac{h}{l}\right)^2\frac{1}{2(\Delta X_e\Delta X_w)}T_j(Z)-\frac{Re}{4}\frac{h}{l}\frac{\hat{U}}{\Delta X_e+\Delta X_w}\|1,\,0\|\,T_j(Z)] \\ -2V_jT_j(Z)-\iota P_j\frac{Re_s}{2}h\sqrt{D}\,T_j(Z) \end{pmatrix}_P$$
$$+\sum_{j=0}^{m}\left(W_j\left[\frac{1}{2(\Delta X_e+\Delta X_w)\Delta X_e}\left(\frac{h}{l}\right)^2-\frac{Re}{8}\frac{h}{l}\frac{\hat{U}}{\Delta X_e+\Delta X_w}\|0,\,1\|\right]T_j(Z)\right)_E$$
$$+\sum_{j=0}^{m}\left(W_j\left[\frac{1}{2(\Delta X_e+\Delta X_w)\Delta X_w}\left(\frac{h}{l}\right)^2+\frac{Re}{8}\frac{h}{l}\frac{\hat{U}}{\Delta X_e+\Delta X_w}\|2,\,1\|\right]T_j(Z)\right)_W, \tag{12}$$

$$\sum_{j=0}^{m}(V_j[\,T_j'(Z)-\sqrt{D}\,T_j(Z)]-\sqrt{D}\,W_jT_j(Z))_P-\sum_{j=0}^{m}\left(U_j\frac{h}{l}\frac{1}{2(\Delta X_e+\Delta X_w)}T_j(Z)\right)_E$$
$$+\sum_{j=0}^{m}\left(U_j\frac{h}{l}\frac{1}{2(\Delta X_e+\Delta X_w)}T_j(Z)\right)_W=0, \tag{13}$$

while the other two Navier-Stokes equations are not given here for brevity. In the above equations, the prime and the double prime denote, respectively, the first and second derivatives with respect to the coordinates concerned; for example, $\hat{U}'=\partial\hat{U}/\partial Z$ and $T''=\partial^2T/\partial Z^2$. Also, the boundary conditions may be written as

$$\sum_{j=0}^{m}U_j(X)\,T_j(1)=0,$$
$$\sum_{j=0}^{m}U_j(X)\,T_j(-1)=0,$$
$$\sum_{j=0}^{m}V_j(X)\,T_j(1)=\hat{e}_r(X),$$
$$\sum_{j=0}^{m}V_j(X)\,T_j(-1)=0,$$
$$\sum_{j=0}^{m}W_j(X)\,T_j(1)=-\hat{e}_r(X),$$
$$\sum_{j=0}^{m}W_j(X)\,T_j(-1)=0. \tag{14}$$

In the present analysis, a system of linear algebraic equations can be obtained by imposing the above equations on the finite number of collocations points in the computational domain $(Z,\,\Theta)$, and applying the equations to a finite number of grid points distributed in the axial domain. As a result, the system of equations can be expressed, as a block-tridiagonal system, in the general form

$$S\Delta Q=R, \tag{15}$$

where ΔQ and R are the vectors for the unknown coefficients and the boundary conditions, respectively. The matrix S represents the block-tridiagonal matrix expressed as

$$S=\begin{bmatrix} P_1 & W_1 & 0 & 0 & 0 & 0 & 0 & 0 \\ E_2 & P_2 & W_2 & 0 & 0 & 0 & 0 & 0 \\ 0 & E_3 & P_3 & W_3 & 0 & 0 & 0 & 0 \\ 0 & 0 & \cdot & \cdot & \cdot & 0 & 0 & 0 \\ 0 & 0 & 0 & \cdot & \cdot & \cdot & 0 & 0 \\ 0 & 0 & 0 & 0 & E_{t-2} & P_{t-2} & W_{t-2} & 0 \\ 0 & 0 & 0 & 0 & 0 & E_{t-1} & P_{t-1} & W_{t-1} \\ 0 & 0 & 0 & 0 & 0 & 0 & E_t & P_t \end{bmatrix}, \quad (16)$$

where E_i, P_i and W_i are matrices of order $2\times[(m-1)+3\times(m+1)]$, concerned with the ith grid point, and the subscript t denotes the number of total grid points considered. Each row of the matrix is concerned with three grid points based on the finite-difference method, and the submatrices are related to the corresponding collocation points based on the spectral method.

When the smooth variations of fluid quantities along the axial direction are expected, it is convenient to have uniformly distributed grid points, $\Delta X_e=\Delta X_w$. In the present analysis with the flexible cylinder, which has small amplitude oscillation, it is possible to use the uniform mesh space. With this step size, the submatrix can be expressed as

$$\begin{aligned} &E_1=E_2=E_3=\cdots=E_t, \\ &P_1=P_2=P_3=\cdots=P_t, \\ &W_1=W_2=W_3=\cdots=W_t. \end{aligned} \quad (17)$$

Therefore, the storage required for the system equations can be reduced.

To obtain the numerical solution, the LU decomposition method is utilized, as mentioned before. The LU decomposition method, which is one of the direct methods, gives the solution in a finite and predeterminable number of operations. This method has proven to be a very useful and efficient tool for solving the block-tridiagonal system of equations.

2.3 Stress componenents and formulation of fluid-dynamic forces

In order to formulate the fluid-dynamic forces acting on the moving cylinder, the stress components including the unsteady pressure, generated by the flexural motion, are considered. By circumferential line integration of the stress components, the unsteady fluid-dynamic forces are obtained. The analysis has now been suffciently progressed to evaluate the unsteady lateral forces.

The resulting fluid-dynamic forces, acting on the cylinder in the direction of oscillatory motion can be calculated by the following equation.

$$F_I(x,\ t)=\int_0^{2\pi} a\Big(\tau_{rr}|_{r=a}\cos\Theta-\tau_{r\theta}|_{r=a}\sin\Theta + \tau_{rx}|_{r=a}\frac{de_I}{dx}\Big)d\Theta, \quad (18)$$

where the stresses are expressed as

$$\begin{aligned} \tau_{rr}(x,\ r,\ \Theta,\ t)&=-p^*+2\mu\frac{\partial v^*}{\partial r}, \\ \tau_{r\theta}(x,\ r,\ \Theta,\ t)&=\mu\Big\{\frac{\partial w^*}{\partial r}+\frac{w^*}{r}+\frac{1}{r}\frac{\partial v^*}{\partial\Theta}\Big\}, \\ \tau_{rx}(x,\ r,\ \Theta,\ t)&=\mu\Big\{\frac{\partial u^*}{\partial r}+\frac{\partial v^*}{\partial x}\Big\}, \end{aligned} \quad (19)$$

The integral effect of the stress component τ_{rx}, acting in x-direction on a surface whose norml vector points in r-direction, on the fluid-dynamic forces is null.

Using the same procedure as in the previous paper (Sim and Cho, 1993) for viscous fluid, the resulting forces can be expressed as

$$F_I(x,\ t)=\rho\pi a^2\omega^2 a\,\hat{e}_{1/2}\Big\{\Re[\hat{F}(x)] + \iota\Im[\hat{F}(x)]\Big\}e^{\iota\omega t}, \quad (20)$$

where the nondimensional fluid-dynamic force, $\hat{F}(x)$, in complex form, is

$$\hat{F}(x)=-\sum_{j=0}^{m}\Big\{P_j(x)+\frac{\iota}{Re_s}[\,V_j^{\dagger}(x)-W_j^{\dagger}(x) + W_j(x)-V_j(x)\Big\}T_j(1), \quad (21)$$

in which

$$\begin{aligned} V_j^{\dagger}(x)&=\frac{8}{hc_j}\sum_{q=j+1}^{m-1} qV_q(x),\ j+q=\text{odd}, \\ W_j^{\dagger}(x)&=\frac{8}{hc_j}\sum_{q=j+1}^{m-1} qW_q(x),\ j+q=\text{odd}, \end{aligned} \quad (22)$$

where $c_0=2$ and $c_j=1(j>0)$. The real and imaginary components of the resulting forces, shown in the above equation are in-phase and in quadrature with displacement, respectively.

2.3 Numerical results

In order to show the rate of convergence of the

numerical solution, the calculations have been conducted for various mesh spacings defined for the finite-difference method. For self-excited flexural motion, it is of interest to estimate the fluid dynamic forces acting on a slender cylinder. In the present work, the length-to-radius ratio remains constant, $l=L/a=15$. Taking account of the nondimensional governing Eqs. (9) and (10), the nondimensional fluid variables are influenced by the Reynolds number Re, as well as by the oscillatory Reynolds number Re_s.

The variation of the calculated fluid dynamic forces with various mesh spacings between two grid points is shown for the case of $b/a=1.05$, $Re=300$ and $Re_s=5{,}000$ in Fig. 2 (the results are obtained with $m=8$). The results at certain grid points ($X=x/L=0.25$, 0.5 and 0.75) are presented. As the spacing is decreased, the results appear to converge to a certain value, and then abruptly diverge. The character of these results might be caused by a truncation error for coarse mesh spacings and by a round-off error for fine mesh spacings. Considering these results, the suitable mesh spacing for the given problem can be selected. For the present case, the optimized spacing should be $\Delta X=0.1$.

Typical results of the nondimensional amplitude of the unsteady velocities across the annular space are shown in Fig. 3(a, b, c) for the case of $b/a=1.25$, $Re=626$ and $Re_s=5{,}000$ with $m=8$ at $X=0.3$, 0.5 and 0.7. The distribution of the real parts of complex-velocity in the circumferential directien has a parabolic shape of low value of Re_s, which is not shown here for brevity. By inspection of Eqs. (20) and (21), the nondimensional pressure $\bar{p}=p^*/(\rho a^2\omega^2 a\hat{e}_{1/2}e^{i\omega t})$ has almost the same order of magnitude as the forces; however, it is found that the skin-friction force become larger as the oscillatory Reynolds number is increased. The interested reader is referred to the pressure distribution along the circumferential direction, shown in the previous work (Sim and Cho, 1993) for translation motion without axial steady flow.

The influene of the Reynolds number ($Re=0$, 626 and 1,256) on the forces along the axial direction is presented in Fig. 4 for $b/a=1.25$ and

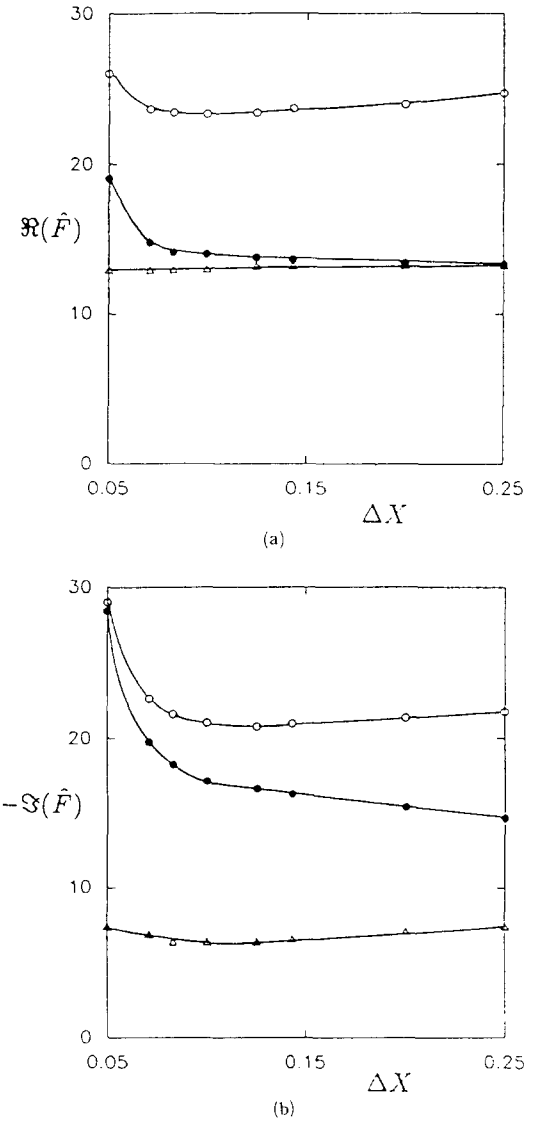

Fig. 2 Variation of (a) the real and (b) the imaginary components of the nondimensional fluid-dynamic forces versus the mesh space ΔX for $b/a=1.05$, $Re=300$ and $Re_s=5{,}000$ ($m=8$) at various axial positions: ●, $X=x/L=0.25$; ○, $X=0.5$; △, $X=0.75$

$Re_s=5{,}000$ for a mesh spacing $\Delta X=0.1$. It is found that the real component of fluid dynamic forces is only slightly dependent on the Reynolds number; however, the imaginary one is strongly influenced by the Reynolds number. As shown in the figure, it is obvious that the real components

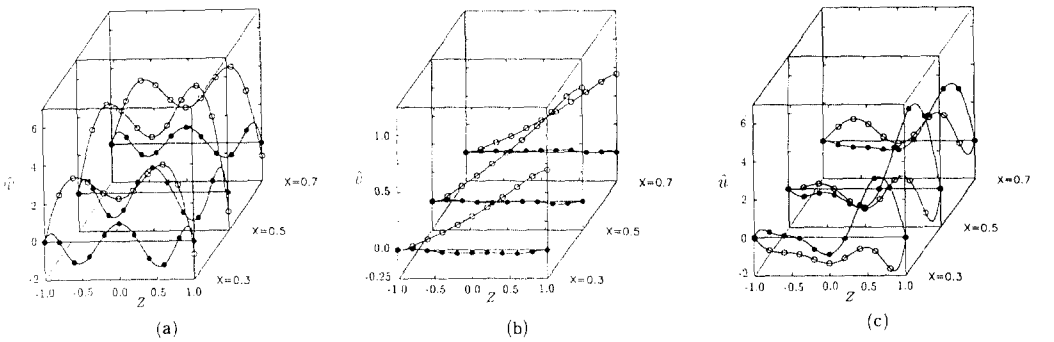

Fig. 3 The nondimensional amplitude distribution of the unsteady flow velocities for $b/a=1.25$, $Re=626$ and $Re_s=5{,}000$ across the annular space ; (a) the circumferential, (b) radial and (c) axial components. ○, real part ; ●, imaginary part

are proportional to the acceleration of the moving cylinder, mainly influenced by the inertia force. The damping forces, related with the imaginary component, might be caused by the combined effects of the unsteady viscous drag and the equivalent Coriolis force. For flexural motion in the first mode, the viscous drag and the Coriolis terms are symmetric and antisymmetric with respect to the middle ($X=1/2$), respectively-since, the former is in phase with displacement of the

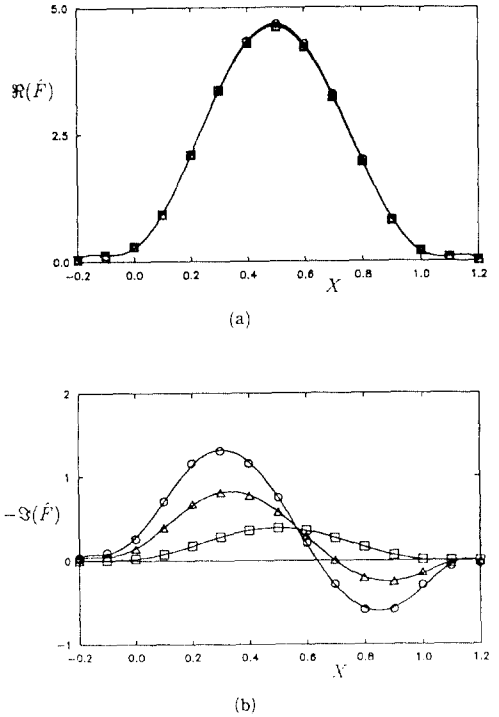

Fig. 4 Influence of axial flow velocity on (a) the real and (b) the imaginary components of the nondimensional fluid-dynamic forces for $b/a=1.25$, $L/a=15$, and $Re_s=5{,}000$ with $\Delta X=0.1$: □, $Re=0$; △, $Re=626$; ○, $Re=1{,}256$

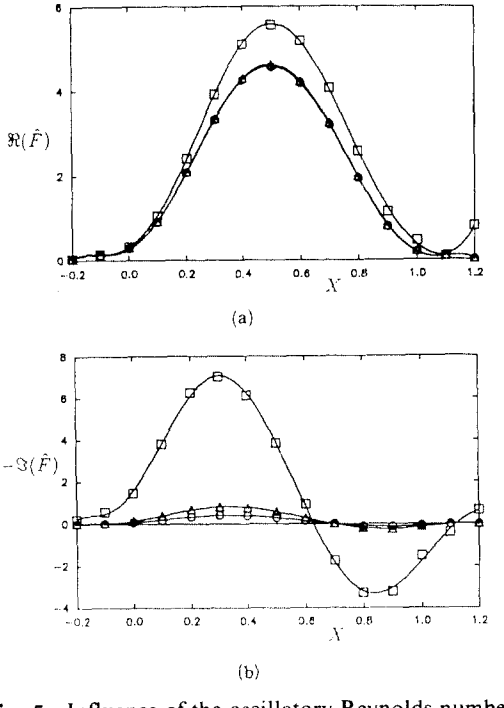

Fig. 5 Influence of the oscillatory Reynolds number on (a) the real and (b) the imaginary components of the nondimensional fluid-dynamic forces for $b/a=1.25$, $L/a=15$, and $Re=626$ with $\Delta X=0.1$: □, $Re_s=500$; △, $Re_s=5{,}000$; ○, $Re_s=10{,}000$

cylinder, while the other is proportional to the first derivative of the displacement. With increasing the Reynolds number (i. e., increasing axial flow velocity), the equivalent Coriolis term becomes larger.

Calculations have been conducted to investigate the effect of the oscillatory Reynolds number (Re_s=500, 5,000 and 10,000) for b/a=1.25, Re =626 with ΔX=0.1 and m=6. The results are show in Fig. 5. For the low value of Re_s=500, the effect on the real part of force (including the viscous effect) is relatively large. The ratio of the imaginary component to the real one becomes smaller with increasing oscillatory Reynolds number ; its effect on the forces is less than 15% in the case of b/a=1.25 with Re_s=5,000 or 10,000. However, the viscous effect on the damping force is important for very narrow annular configurations.

3. Approximate Semi-Analytical Method

The numerical results obtained in the previous section will be compared to the approximate results obtained in this section. This is one of the necessary procedures to validate the newly developed numerical method, since there are no other previous results to be used for comparison. For this purpose, the approximate analytical method (Païdoussis, et al., 1990) will be modified to obtain an improved unsteady viscous flow solution.

The fluid-dynamic forces are formulated, first assuming the case of an unsteady potential (inviscid) flow, and then considering also the main effects of fluid viscosity. The unsteady inviscid force will be obtained by the numerical approach based on the spectral method with the aid of the separation of variables method, which is more rigorous than the previous analytical method ; however, the viscous effects are approximated analytically by the same principles as in the reference (Païdoussis, et al., 1990). This is the reason why the method is called semi-analytical. The present semi-analytical results are also compared to ones obtained by he previous analytical method especially for narrow annular configurations.

Based on the assumption of small amplitude oscillations of the flexible centrebody in an annulus, the two flow fields, potential and viscous, are considered to simplify the approach of this problem. The unsteady viscous forces are formulated by considering the mean circumferential flow velocity obtained by potential flow theory. The direction of the mean flow velocity, which is considered to oscillated, is then determined, and the unsteady viscous pressure drop along the circumferential direction and the shear stress acting on the wall are evaluated.

The axial steady flow is assumed to be a fully developed laminar flow characterized by the mean flow velocity $\bar{U}$, static pressure P_∞ and the fluid density ρ, which is considered constant.

3.1 Derivation of the inviscid force

With no separation in the annular flow, the inviscid forces are derived by potential flow theory. For incompressible fluid, the unsteady governing equation is expressed in terms of the unsteady velocity potential ϕ, in the form of the Laplace equation :

$$\nabla^2\phi=\frac{\partial^2\phi}{\partial x^2}+\frac{\partial^2\phi}{\partial r^2}+\frac{1}{r}\frac{\partial\phi}{\partial r}+\frac{1}{r^2}\frac{\partial^2\phi}{\partial\Theta^2}=0, \tag{23}$$

subjecto to the boundary conditions

$$\left.\frac{\partial\phi}{\partial r}\right|_{r=a}=\frac{\partial e_r}{\partial t}+\left[\frac{\partial\phi}{\partial x}\frac{\partial e_r}{\partial x}+\frac{1}{r}\frac{\partial\phi}{\partial\Theta}\frac{1}{r}\frac{\partial e_r}{\partial\Theta}\right],$$
$$\left.\frac{\partial\phi}{\partial r}\right|_{r=b}=0,\ \left.\frac{\partial\phi}{\partial x}\right|_{x=-\infty}=\bar{U}, \tag{24}$$

where the radial displacement, $e_r(x, \Theta, t)$, is expressed in terms of the eigenfunctions, ψ_k, of the corresponding beam-see the reference (Païdoussis, et al., 1990).

Using the separation of variables method, the velocity potential $\phi(x, r, \Theta, t)$ may be written in the form

$$\phi(x, r, \Theta, t)=\sum_k a_k\hat{\phi}_k(x, r)\cos\Theta e^{i\omega t}, \tag{25}$$

where the reduced potentials $\hat{\phi}_k(x, r)$ can be expressed as

$$\hat{\phi}_k(x, Z)=f_k(x)F_k(Z), \tag{26}$$

in terms of new coordinate $Z=1-2(r-a)/H$.

Taking into account the coordinate transformation, the reduced potentials, $\hat{\phi}_k(x, Z)$, i.e.

$$\frac{a^2h^2}{4}\frac{\partial^2\hat{\phi}_k}{\partial x^2}+\frac{\partial^2\hat{\phi}_k}{\partial Z^2}-\sqrt{D}\frac{\partial\hat{\phi}_k}{\partial Z}-D\hat{\phi}_k=0, \tag{27}$$

with the boundary conditions

$$\left.\frac{\partial\hat{\phi}_k}{\partial Z}\right|_{Z=-1}=0,$$
$$\left.\frac{\partial\hat{\phi}_k}{\partial Z}\right|_{Z=1}=-\frac{ah}{2}[\iota\omega\psi_k(x)+\bar{U}\psi_k'(x)], \tag{28}$$

where the prime denotes differentiation with respect to x, the nondimensional annular space is expressed as $h=(b-a)/a=H/a$. As compared to the previous analysis (Païdoussis, et al., 1990), it is obvious that this potential theory is not restricted to very narrow annuli. Considering the normal mode expansion for the motion of cylinder, which can be separated into trigonometric and hyperbolic components, it is more convenient to define the reduced-motion potentials, $\hat{\phi}_{1k}$ and $\hat{\phi}_{2k}$, as follows:

$$\hat{\phi}_k(x, Z)=\sum_{s=1}^{2}f_{sk}(x)F_{sk}(Z)$$
$$=\hat{\phi}_{1k}(x, Z)+\hat{\phi}_{2k}(x, Z), \tag{29}$$

where

$$\hat{\phi}_{1k}(x, Z)=[A_a\cos\beta_kx+A_b\sin\beta_kx]\sum_j\hat{\Phi}_{1kj}T_j(Z),$$
$$\hat{\phi}_{2k}(x, Z)=[B_a\cosh\beta_kx+B_b\sinh\beta_kx]$$
$$\sum_j\hat{\Phi}_{2kj}T_j(Z),$$

in terms of the eigenvalues, β_kL, of the eigenfunctions and the expansion forms of Chebyshev polynomials, $T_j(Z)$. In the above equations, the subscripts 1 and 2, stand for the trigonometric and hyperbolic terms, respectively.

Substituting the reduced-motion potentials into the governing equation leads to

$$\sum_{j=0}^{m}\hat{\Phi}_{ikj}T_j''(Z)-\sqrt{D}\,\hat{\Phi}_{ikj}T'(Z)-\left[D\pm\left(\frac{ah\beta_k}{2}\right)^2\right]$$
$$\hat{\Phi}_{ikj}T_j(Z)=0, \tag{30}$$

subject to the boundray conditions

$$\sum_{j=0}^{m}\sum_{s=1}^{2}f_{sk}(x)\hat{\Phi}_{skj}T_j'(-1)=0,$$

$$\sum_{j=0}^{m}\sum_{s=1}^{2}f_{sk}(x)\hat{\Phi}_{skj}T_j'(1)$$
$$=-\frac{ah}{2}\sum_{s=1}^{2}[\iota\omega\psi_{sk}(x)+\bar{U}\psi_{sk}'(x)], \tag{31}$$

where the two sets of solutions, $s=1$ and 2, arising from $+\beta_k^2$ and $-\beta_k^2$ in the above equations can each be associated with either ψ_{1k} or ψ_{2k}, defined for the trigonometric and hyperbolic components of the eigenfunctions, respectively.

Considering the $+\beta_k^2$ case for the trigonometric components, the boundary conditions can be rewritten

$$-\frac{ah}{2}[\iota\omega\psi_{1k}(x)+\bar{U}\psi_{1k}'(x)]$$
$$=[A_a\cos\beta_kx+A_b\sin\beta_kx]\sum_{j=0}^{m}\hat{\Phi}_{1kj}T_j'(1), \tag{32}$$

through which the constants, A_a, and A_b, may be determined. Proceeding similarly, the constants, B_a and B_b associated with $-\beta_k^2$, may also be determined. Hence, the unknown constants are found to be

$$A_a=-\frac{ah}{2}[-\iota\omega+\bar{U}\sigma_k\beta_k],$$
$$A_b=-\frac{ah}{2}[\iota\omega\sigma_k+\bar{U}\beta_k],$$
$$B_a=-\frac{ah}{2}[\iota\omega-\bar{U}\sigma_k\beta_k],$$
$$B_a=-\frac{ah}{2}[-\iota\omega\sigma_k+\bar{U}\beta_k], \tag{33}$$

and the boundary conditions are reduced to

$$\sum_{j=0}^{m}\hat{\Phi}_{skj}T_j'(1)=1,\ \sum_{j=0}^{m}\hat{\Phi}_{skj}T_j'(-1)=0, \tag{34}$$

where $\sigma_k=(\cosh\beta_kL-\cos\beta_kL)/(\sinh\beta_kL-\sin\beta_kL)$, the β_kL being the corresponding eigenvalues of a clamped-clamped beam.

Imposing the governing Eq. (30) at a finite number $(m-1)$ of collocation points, equally distributed in the radial direction and considering the above boundary condition, the solution of the reduced potential $\hat{\phi}_k$ can be completely the determined from algebraic equation obtained. Thus, the reduced potential can be evaluated on the surface of the moving cylinder $(Z=1)$:

$$\hat{\phi}_k(x, 1)=-a\sum_{s=1}^{2}G_{sk}[\iota\omega\psi_{sk}(x)+\bar{U}\psi_{sk}(x)], \tag{35}$$

where

$$G_{1k}=\frac{h}{2}\sum_{j=0}^{m}\hat{\Phi}_{1kj},\quad G_{2k}=\frac{h}{2}\sum_{j=0}^{m}\hat{\Phi}_{2kj}. \tag{36}$$

Substituting the solution of the unsteady velocity potential into the unsteady Bernoulli equation, $P-P_\infty=\frac{1}{2}\rho\bar{U}^2-\frac{1}{2}\rho|\nabla(\phi_s+\phi)|^2-\rho\frac{\partial\phi}{\partial t}$, with the aid of $d\phi_s/dx=\bar{U}$ and integrating around the circumference of the inner cylinder, the unsteady inviscid force is found to be

$$\begin{aligned}F_p(x,\ t)&=-\int_0^{2\pi}a(P-P_\infty)|_{r=a}\cos\Theta d\Theta\\&=-\rho\pi a^2e^{\iota\omega t}\sum_k a_k(-\omega^2P_{k2}+\iota\omega P_{k1}\\&\quad+P_{k0}),\end{aligned} \tag{37}$$

where

$$\begin{aligned}&P_{k2}=\sum_{s=1}^{2}G_{sk}\psi_{sk},\ P_{k1}=2\bar{U}\sum_{s=1}^{2}G_{sk}\psi'_{sk},\\&P_{k0}=\bar{U}^2\beta_k^2\sum_{s=1}^{2}(-1)^sG_{sk}\psi_{sk}.\end{aligned} \tag{38}$$

The inviscid forces are expressed as the general form : The added mass χ is dependent only on the cross sectional geometry for slender body (Paîdoussis, 1973). However, in the present theory being applicable to cylinders of small length-to-radius ratio, the added mass is dependent on the eigenfunctions of the beam as well as the geometry, as described in the above equation. Therefore, G_{sk} are equivalent added mass coefficients in this analysis.

3.2 Determination of the viscous forces

As shown in the simplified unsteady viscous model (Paîdoussis, et al., 1990), perturbation terms due to unsteady viscous effects are superimposed on the unsteady terms obtained above ; thus, the nondimensional pressure perturbation with respect to $\rho\bar{U}^2$ is defined by

$$\tilde{p}\ (x,\ r,\ \Theta,\ t)=\tilde{p}_v(x,\ r,\ \Theta,\ t)+\tilde{p}_p(x,\ r,\ \Theta,\ t), \tag{39}$$

and simlarly, for the nondimessional velocity components with respect to the mean axial flow velocity, $\tilde{u}$, $\tilde{v}$ and $\tilde{w}$, where the components, $\tilde{u}_v$, $\tilde{v}_v$, $\tilde{w}_v$, and $\tilde{p}_v$, associated with viscous effects are considered to depend only slightly on Θ and t.

It was found in the simplified unsteady viscous model that, for laminar flow, the gradient of the pressure perturbation $\tilde{p}_v$ due to the unsteady viscous effect is expressed as

$$\frac{\partial\tilde{p}_v}{\partial\xi}=-\frac{24}{h}\frac{1}{Re}=-\frac{c_f}{h}\simeq\frac{\partial P_m}{\partial x}\frac{a}{\rho\bar{U}^2}, \tag{40}$$

where P_m denotes mean pressure, the nondimensional friction coefficient c_f is defined by

$$c_f=\frac{24}{Re}, \tag{41}$$

and $Re=\rho\bar{U}D_H/\mu$ is the Reynolds number based on the hydraulic diameter $D_H=2ha$. In the above equation, ξ is a coordinated directed by the total mean flow velocity, which fluctuates circumferentially through a small angle ϑ calculated as

$$\begin{aligned}\sin\vartheta=\bar{w}&=\frac{1}{H}\int_{r=a}^{r=b}\tilde{w}dr\\&=\sum_k\frac{a_k}{2\bar{U}}\left[\sum_{s=1}^{2}f_{sk}W_{sk}\right]\sin\Theta e^{\iota\omega t},\end{aligned} \tag{42}$$

where

$$f_{sk}=G_{sk}[\iota\omega\psi_{sk}(x)+\bar{U}\psi'_{sk}(x)],$$

and

$$W_{sk}=\sum_{j=0}^{m}\int_1^1\frac{2}{2-h(Z-1)}\hat{\Phi}_{skj}T_j(Z)dZ.$$

The dimensional shear stress on the cylinder in the circumferential direction is found to be

$$\tau_\Theta=\tau\sin\vartheta, \tag{43}$$

where

$$\tau=\rho\bar{U}^2\frac{12}{Re}=c_f\frac{1}{2}\rho\bar{U}^2.$$

Now, the unsteady lateral viscous force F_{vl} can be evaluated

$$\begin{aligned}F_{vl}&=-\int_0^{2\pi}[\tau_\Theta\sin\Theta+\rho\bar{U}^2\tilde{p}_v\cos\Theta]ad\Theta\\&=-\rho\pi a^2e^{\iota\omega t}\sum_k a_k(\iota\omega\bar{P}_{k1}+\bar{P}_{k0}),\end{aligned} \tag{44}$$

where

$$\begin{aligned}&\bar{P}_{k1}=-\frac{c_f\bar{U}}{2}\frac{2+h}{ah^2}\sum_{s=1}^{2}G_{sk}W_{sk}\psi_{sk},\\&\bar{P}_{k0}=-\frac{c_f\bar{U}^2}{2}\frac{2+h}{ah^2}\sum_{s=1}^{2}G_{sk}W_{sk}\psi'_{sk}.\end{aligned} \tag{45}$$

By inspection of the above equation, it is clear that the lateral viscous forces are dependent on the Reynolds number ($c_f=24/Re$) and the geometry of the system : The effect of the pressure perturbation is $2/h$ times that of the shear stress.

considering the numerator, $2+h$.

Considering the inviscid and lateral viscous forces without taking into account the steady longitudinal force, the fluid-dynamic forces are expressed in comples form as

$$F=F_p+F_{vl}$$
$$=\rho\pi a^2\omega^2 a_1\psi_1(L/2)e^{\iota\omega t}[\Re(\hat{F})+\iota\Im(\hat{F})], \quad (46)$$

where $a_1\psi_1(L/2)e^{\iota\omega t}$ denotes the lateral displacement of the moving cylinder at $x=L/2$.

3.3 Comparison with previous solution

The equivalent added mass coefficients defined in Eq. (36), G_{sk} can be predicted by the present theory and then will be compared with those obtained by the previous theory (Païdoussis, et al., 1990) for situations where both should be applicable. The equivalent added mass coefficients obtained by the present inviscid flow theory are presented for slender cylinders ($l=L/a=20$) with radius ratios, $b/a=1.05$ and $1.1(m=6)$. As shown in Table 1, it is seen that better agreement is for a narrower annulus ($b/a=1.05$), where the narrow-annulus simplification of the previous theory applies best. The added mass coefficients obtained by slender body theory (Païdoussis, 1973), $\chi=[(1+h)^2+1]/[(1+h)^2-1]$, are also presented to compare with the results (χ is independent on the eigenfunctions as compared to the present results).

Before comparing the present approximate results to the numerical results, the nondimensional fluid-dynamic forces, $\Re(\hat{F})$ and $\Im(\hat{F})$, obtained by the present approximate method are compared with those of the previous approximated analytical method for $l=15$ and $Re_s=5,000(m=6)$. In Fig. 6, the result is calculated for for $b/a=1.1$ and $Re=400$. It is found that the discrepancy is very small for the narrower case,

Table 1 Comparison of equivalent added mass coefficients for concentrically narrow annular flow; $l=L/a=20$, (a) $b/a=1.05$ and (b) $b/a=1.1$

	Previous Results(1)		Present Results(2)		Rel. Difff(%) [(2)−(1)]/(2)	
k	G_{1k}	G_{2k}	G_{1k}	G_{2k}	ΔG_{1k}	ΔG_{2k}
1	18.49	20.68	19.38	21.79	4.5	5.1
2	16.92	23.08	17.66	24.47	4.2	5.2
3	14.99	27.97	15.57	30.05	3.7	6.9

$\chi=20.51$

(a)

	Previous Results(1)		Present Results(2)		Rel. Difff(%) [(2)−(1)]/(2)	
k	G_{1k}	G_{2k}	G_{1k}	G_{2k}	$1k$	$2k$
1	9.04	10.11	9.92	11.21	8.8	9.9
2	8.27	11.28	9.00	12.67	8.1	11.0
3	7.34	13.66	7.90	15.76	7.2	13.3

$\chi=10.52$

(b)

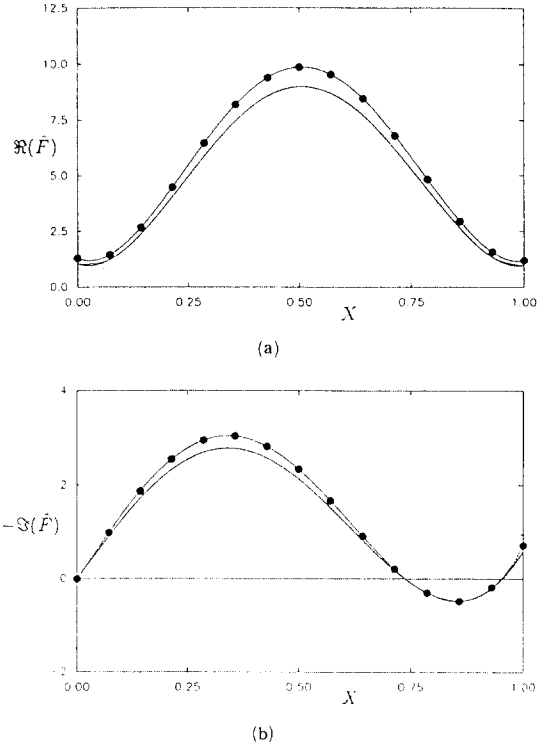

Fig. 6 Comparison of (a) the real and (b) the imaginary components of the nondimensional fluid-dynamic forces for $b/a=1.1$, $L/a=15$, $Re=400$ and $Re_s=5,000$, obtained by two methods: — ● —, the present semi-analytical method; —, the previous analytical method

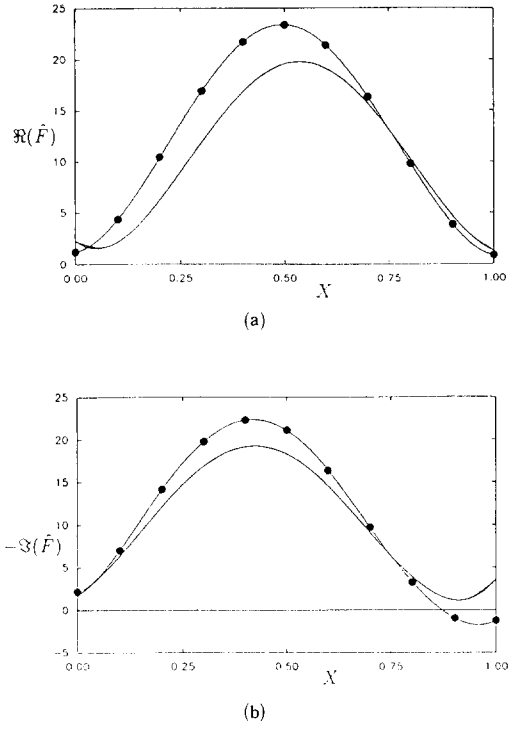

Fig. 7 Comparison of (a) the real and (b) the imaginary components of the nondimensional fluid-dynamic forces for $b/a=1.05$, $L/a=15$, $Re=300$ and $Re_s=5{,}000$, obtained by two methods : — ● —, the numerical method ; —, the semi-analytical method

where the both theories are quite applicable. Hence, the present approximate results can be compared with confidence to the present numerical results obtained in Section 2.

The present approximate results are compared to the numerical result with $\Delta X=0.1$ and $m=7$ for $b/a=1.05$, $Re=300$ and $Re_s=5{,}000$, where the two theory can be applicable. Good agreement between two results is shown in Fig. 7. Even for a high oscillatory Reynolds number ($Re_s=5{,}000$), the viscous damping force is important for very narrow annular configurations.

4. Conclusions

Using the collocation the moving cylinder, systematically. The fluid dynamic force is dependent on the oscillatory Reynolds number as well as the Reynolds number. However, the results cannat be expressed in term of the osclillatory motion of cylinder explicitly, which would be desirable for the stability analysis of the system.

The strength of the present semi-analytical theory is that the unsteady inviscid forces are predicted numerically without the limitation, shown in the previous analytical theory, of a narrow annular space. Thus, for the system where unsteady inviscid forces are dominant over fluid-dynamic forces, the semi-analytical theory is fairly applicable, even if in case of a finite length of cylinder and a slightly confined flow. The viscous effects on the fluid-dynamic forces for narrow annular configurations can be estimated by the present approximate method.

A number of significant observations may be made from the results. First, with increasing axial flow velocity, the Coriolis term, which is associated with the antisymmetric component of the damping forces with respect to $X=1/2$ in the present work, becomes larger, almost linearly with flow velocity. This could be important for wave propagation studies. The second point of interest is that the fluid-dynamic forces for relatively wide annuli with high oscillatory Reynolds number can be estimated by potential flow theory : the viscous effect can be negligible in this case. However, for very narrow annuli, the damping forces are stronger. These significant damping forces are mainly caused by the unsteady viscous drag, which is more or less linearly dependent on the amplitude of oscillatory motion. Finally, the effect of the unsteady pressure perturbation on the fluid-dynamic forces becomes dominant with respect to the shear stress effect with decreasing annular space.

References

Chen, S. S., 1981, "Fluid Damping for Circular Cylindrical Structures," Nuclear Engineering and Design, Vol. 63(1), pp. 81~100.

Lighthill, M. J., 1960, "Note on the Swimming of Slender Fish," Journal of Fluid Mechanics, Vol. 9, pp. 305~317.

Mateescu, D., Païdoussis, M. P. and Sim,

W.-G., 1990, "CFD Solution for Steady Viscous and Unsteady Potential Flow between Eccentric Cylinders," ASME International Symposium on Nonsteady Fluid Dynamics, Toronto, FED-Vol. 92, pp. 235~242.

Païdoussis, M. P., 1966a, "Dynamics of Flexible Slender Cylinders in Axial Flow ; Part I : Theory," Journal of Fluid Mechanics, Vol. 26, pp. 717~751.

Païdoussis, M. P., 1973, "Dynamics of Cylindrical Structures Subjected to Axial Flow," Journal of Sound and Vibration, Vol. 29(3), pp. 365~385.

Païdoussis, M. P. and Pettigrew, M. J., 1979, "Dynamics of Flexible Cylinders in Axisymmetrically Confined Axial Flow," Journal of Applied Mechanics, Vol. 46, pp. 37~44.

Païdoussis, M. P., 1987, "Flow-induced Instabilities of Cylindrical Structures," ASME Applied Mechanics Reviews, Vol. 40(2), pp. 163~175.

Païdoussis, M. P., Mateescu, D. and Sim, W-G., 1990, "Dynamics of stability of a Flexible Cylinders in a Narrow Coaxial Cylindrical Dust Subjected to Annular Flow," Journal of Applied Mechanics, Vol. 57, pp. 232~240.

Patanker, S. V., 1980 "Numerical Heat Transfer and Fluid flow," McGraw-Hill Book Co., New York.

Sim, W.-G. and Cho, Y.-C., 1993, "Unsteady Potential and Viscous Flows between Eccentric Cylinders," KSME Journal, Vol. 7(1), pp. 55~69.

Spalding, D. B., 1972, "A Novel Finite-difference Formulation for Differential Expressions Involving both First and Second Derivatives," International Journal for Numerical Method in Engineers, Vol, 4, pp. 551~559.

Taylor, G. I., 1952, "Analysis of the Swimming of long and Narrow Animals," Proceedings of the Royal Society (London). A214, pp. 158~183.